Experimental Investigations On Optimizing Manufacturing Parameters For Electro-Spark Deposition Diamond Wire Saw

Chengyun Li
Shandong University
Peiqi Ge (pqge@sdu.edu.cn)
Shandong University
Wenbo Bi
Shandong University
Qihao Wang
Shandong University

Research Article

Keywords: Diamond wire saw (DWS), Electro-spark deposition (ESD), Orthogonal experiments, Extremum difference analysis

Posted Date: December 29th, 2021

DOI: https://doi.org/10.21203/rs.3.rs-1194110/v1

Abstract

The third generation of superhard semiconductor materials, represented by single-crystal SiC, is used widely in microelectronics due to their excellent physical and mechanical properties. However, their high hardness and brittleness become the bottleneck of their development. Diamond wire saw (DWS) has become the mainstream tool for sawing hard and brittle crystal materials. However, the diamond abrasive is consolidated on the core wire through resin or electroplated nickel, and the holding strength is not high. When sawing superhard crystal materials, the efficiency is low. In order to improve the sawing efficiency of superhard crystal materials, it is of great significance to improve the wear resistance of wire saw and the holding strength of abrasive particles. Electro-spark deposition (ESD) can deposit electrode materials on the substrate with low heat input to achieve metallurgical bonding between metal materials. It can effectively improve the gripping strength of the abrasive grains. And the sawing ability of the wire saw to make the consolidated DWS by the ESD process. In this paper, the ESD equipment has been designed according to the characteristics of the ESDDWS process. The discharge gap size and electrode consumption are monitored in real-time by a single-chip microcomputer (SCM). Orthogonal experiments were carried out for the two motion modes. The effects of process parameters, such as (A) Grain size, (B) Abrasive content, (C) Pulse duration time, (D) Compacting pressure, (E) Current, (F) Electrode diameter, (G) Pulse interval time, (H) Reciprocating times, (I) Wire feed speed, on the quality of ESDDWS were analyzed. Through the extremum difference analysis, the optimal parameter combinations of ESDDWS were obtained. The results of the validation experiment are better than the original experimental results.

1 Introduction

The third-generation semiconductor materials (such as SiC and GaN) have the characteristics of a high breakdown field, great charge carrier saturation, and elevated dissociation temperatures. It can meet the new requirements of modern electronic technology for high temperature, high voltage, high frequency, high power, and radiation resistance [1, 2]. Therefore they have a broad application prospect in the field of microelectronics [3]. However, their high hardness and brittleness become the bottleneck of their development [4].

DWS has become the mainstream tool for slicing hard and brittle materials [5]. At present, DWS mainly includes resin DWS and electroplated DWS [6]. The diamond abrasives are attached to a core wire by resin or electroplated. Diamond abrasive particles are less strongly bonded and have shorter service life due to easy drop-off and wear of the abrasive layer. Slicing the super hard crystal is very difficult and inefficient. In order to improve the slicing efficiency, it is necessary to improve the holding strength and wear resistance of the DWS.

ESD is a deposition process in which the electrode material is deposited on the metal substrate by applying a short duration and high current pulse between cathode and anode. It has become a new surface treatment technique to improve the wear and corrosion resistance of the workpiece. Furutani et al. has proposed the manufacturing technology of wire saw by EDM. At first, they used suspending Ti

powder to make a saw wire with a hard deposition tumor, which can be used to cut copper bars and glass. However, this method is difficult to deposit abrasive particles on the core wire [7, 8]. And then, they put forward the electrode made by powder compacted and made a wire saw containing alumina abrasive particles[9–11]. However, they did not make a theoretical analysis on the selection of discharge parameters. And the wire was broken in the experiment. Meanwhile, they did not study the distribution of wear particles on the deposition layer. However, the distribution of abrasives has an important impact on the sawing process.

At present, ESD devices are usually using handheld devices, and the deposition process needs to be adjusted by operators according to experience. It has high labor intensity and low production efficiency. More and more researchers have paid attention to the mechanical automation of ESD [12, 13]. Frangini et al.[14] realized the continuous automatic deposition of large planes by dynamically controlling the contact force. They proposed that the dynamic control of contact force can improve the stability of the ESD process and reduce the influence of roughness on spark reproducibility. Wang et al. [15–17] designed a special tool handle for the ESD process to be connected to the spindle of the milling machine, realized the integration of ESD equipment and CNC milling machine, and controlled the continuous progress of the ESD process through the average loss rate of electrode material. Wang et al. [18] designed a set of ESDDWS equipment to control the continuous deposition by monitoring the average voltage of the discharge gap. However, this method needs a fixed sampling time and can not respond to the conditions in the deposition process in time.

In this article, An ESD equipment is designed according to the characteristics of the ESDDWS process. The discharge gap size is monitored in real-time and adjusted by an SCM. Orthogonal experiments were carried out for the two motion modes. The effects of process parameters, such as (A) Grain size, (B) Abrasive content, (C) Pulse duration time, (D) Compacting pressure, (E) Current, (F) Electrode diameter, (G) Pulse interval time, (H) Reciprocating times, (I) Wire feed speed, on the quality of ESDDWS were analyzed. Through the extremum difference analysis, the optimal parameter combinations of ESDDWS were obtained.

2 Experiment Setup

2.1 ESDDWS deposition equipment

The manufacturing principle of ESDDWS and two motion modes of deposition have been introduced [19, 20]. The deposition device was designed according to the characteristics of the ESDDWS process, as shown in Fig. 1. The device is equipped with two deposition stations for horizontal and vertical deposition. Each deposition station can realize the deposition of two sides of the saw wire. So as to satisfy the deposition of the saw wire from four directions. In this experiment, only one side of the saw wire was deposited to analyze the effect of deposition process parameters on the quality of the deposition layer.

In order to meet real-time detection and response, the limit feedback laser is adopted to detect the discharge gap and electrode consumption. And then the signal feedback to the SCM. The control schematic diagram have been shown [20].

In motion mode 1, the electrode rotates at a uniform speed. Meanwhile, the core wire feeds at a uniform speed. The electrode and the core wire keep a fixed gap. And it is dynamically controlled by the SCM. The motion control flow chart of motion mode 1 is shown in Fig. 2. Pre-setting is required before the program, such as laser position, electrodeposition, program debugging, etc. After starting, the core wire starts to feed first, and then the electrode moves. When the electrode reaches the discharge position, the electrode covers the laser beam, and the signal of the laser receiver changes. The SCM receives the signal and controls the electrode to stop moving. Then the wire and electrode kept a fixed distance to carry out normal deposition. During the deposition process, the electrode material is gradually consumed. The laser receiver signal changes again when the electrode material can not shield the laser beam. Then the SCM controls the motor to adjust the position of the electrode.

In motion mode 2, the electrode rotates and reciprocates intermittently. Meanwhile, the core wire feeds intermittently. The discharge gap and material consumption are also dynamically controlled by the SCM during electrode reciprocation. The motion control flow chart of motion mode 2 is shown in Fig. 3. The pre-setting is also required before the deposition starts. After the program start, the electrodes feed close to the core wire until fed at a fixed distance. Then it reaches the discharge position and begins to deposit. After discharging, the electrode moves backward until the laser signal changes. Then, the electrodes stop the move and rotate at an angle. At the same time, the wire feeds for a distance. Continuous deposition occurs in this cycle. The stepping motor driver model is TS DMA860H, and the electrical parameters are shown in Table 1. The guide of the ball screw is 5mm, so the minimum feed of the electrode is 0.1um. That is, the positioning accuracy of the electrodes is 0.1um. It has met the requirements of the deposition process.

Table 1
Step motor driver parameters

Parameter	Value			
	Min	Typical	Max	Unit
Output current	2.1		7.2	A
Input power voltage	24	48	75	VAC
Control signal input current	6	10	16	mA
Control signal interface voltage	4.5	5	28	VDC
Input signal pulse width	1.5	-	-	μs
Subdivision	400	-	51200	Pulse/rev
Step pulse frequency	0	-	200	KHz

2.2 Experimental parameters setting

In this work, the diamond abrasive grains were chosen W10 and W40, respectively. Generally, the content of components of the mixture is determined by mass percentage. But the density of diamond abrasive particles in DWS is usually measured by quantity. Due to the change of diamond size, the density of diamond abrasive particles in the electrodes varies greatly with the same mass fraction. The density of abrasive particles contained in the melting droplets is too high to cause the accumulation of abrasive particles in the deposition layer. Therefore, the mass fraction is converted into the relationship of the density of abrasive particles (as shown in Eq. 1 to 5).

$$N_{\mathrm{sin\,gle}}=\frac{\mathrm{V_{melt}}\times\rho_{\mathrm{mix}}\times\mathrm{w}_t}{\rho_{diamond}\times V_{diamond}} \quad (1)$$

$$N_{\mathrm{duration}}=N_{\mathrm{discharg\,e}}\times N_{\mathrm{sin\,gle}} \quad (2)$$

$$N_{\mathrm{saw}}=\mathrm{K_{bond}}\times N_{duration} \quad (3)$$

$$\rho_{\mathrm{saw}}=\frac{4N_{\mathrm{saw}}}{\mathrm{L_{dis}}} \quad (4)$$

$$\mathrm{w_t}=\frac{\rho_{saw}\mathrm{L_{dis}}\rho_{diamond}V_{diamond}}{4\mathrm{K_{bond}N_{dis}}charge\rho_{\mathrm{mix}}\mathrm{V_{melt}}} \quad (5)$$

We assume that the amount of abrasive deposited on the surface of the wire after one discharge is 1. And the mass fraction of diamond abrasives in the electrodes is shown in Table 2. The amount of abrasive in the deposited layer is increased due to repeated discharge. Therefore, for W40 abrasives, the density value should be reduced appropriately. However, because the diameter of the W10 abrasive is small, more abrasives need to be used in the same area. Therefore, the mass fractions of the two abrasives are set to 1%, 2%, and 4%, respectively.

Table 2
Abrasive content corresponding to electrode melting volume

Parameter		Value		
Electrode melting volume(μm^3)		384000	640000	960000
Abrasive content(%wt)	W40	6.64	3.99	2.66
	W10	0.1	0.06	0.04

The pressing pressure of green compacted electrodes has an important impact on the deposition quality [21]. The pre-pressing test shows that the electrode often breaks down when the pressing pressure is 100 MPa. Therefore, the pressing pressure of green compacted electrodes is set to 200 MPa, 300 MPa, and 400 MPa, respectively.

At the same time, the discharge area between the electrodes and the wire will affect the uniformity of the deposited layer, considering the randomness of electro spark discharge. In the experiment, the diameters of the electrodes are selected 3mm and 10mm, respectively. In addition, single-point discharge of the substrate and the electrode can be realized by aligning the circumference of the electrode with the core wire, which can be equivalent to the electrode diameter of 0 mm.

Discharge current and pulse duration time have an important influence on the melting amount of electrode material. Moreover, the thickness of the abrasive layer of the diamond wire saw is not as good as the thickness. The proper process parameters must be found so that the abrasive particles on the surface of the saw wire do not accumulate and are well consolidated. According to the research results, the pulse duration time is set to 12 μs, 20 μs, and 30 μs, respectively [20]. In addition, in order to explore the effect of discharge current on deposition quality, the current is carried out at 15A, 19A, and 23A, respectively.

Table 3
Experimental parameter

Parameter		**Value/Lever**		
		1	**2**	**3**
(A) Grain size		W40	W10	
(B) Abrasive content (%wt)		1	2	4
(C) Pulse duration time (μs)		12	20	30
(D) Compacting pressure (MPa)		200	300	400
(E) Current (A)		15	19	23
(F) Electrode diameter (mm)		10	3	0(equivalent)
Move model 1	(G) Pulse interval time (ms)	2	4	8
	Wire feed speed (mm/s)	25		
Move model 2	Pulse interval time (ms)	10		
	(H) Reciprocating times (cycle/step)	1	2	3
	(I) Wire feed speed (mm/step)	0.5	1	2

The effect of pulse interval time on different modes of motion has been studied [20]. In move mode 1, the value of the pulse interval time can be small, but the wire velocity is related to the distance of the adjacent deposition points. Therefore, when setting the pulse interval time, the kinematic performance of the machine tool is taken into account. Theoretically, the spacing should be the diameter of the discharge channel so that adjacent deposition points do not interfere with each other. In practice, the spacing can be reduced appropriately, considering that the deposited material does not cover the entire discharge channel area. That is, the pulse interval time can be reduced appropriately. In the experiment, the velocity

of the wire is set to 25mm/s. And the pulse interval time is set to 2ms, 4ms, 8ms, respectively. In move mode 2, in order to ensure the smooth progress of the experiment, the pulse interval time can be determined to be 10ms based on the simulation results.

In summary, the experimental parameters are shown in Table 3. Orthogonal experiments are performed for the two motion modes, and the orthogonal parameter combinations are shown in Table 4 and Table 5.

Table 4
Orthogonal experimental combination for move modle 1

No.	A	B	C	D	E	F	G
1	W40	1	12	200	15	10	2
2	W40	1	20	300	19	3	4
3	W40	1	30	400	23	0	8
4	W40	2	12	200	19	3	8
5	W40	2	20	300	23	0	2
6	W40	2	30	400	15	10	4
7	W40	4	12	300	15	0	4
8	W40	4	20	400	19	10	8
9	W40	4	30	200	23	3	2
10	W10	1	12	400	23	3	4
11	W10	1	20	200	15	0	8
12	W10	1	30	300	19	10	2
13	W10	2	12	300	23	10	8
14	W10	2	20	400	15	3	2
15	W10	2	30	200	19	0	4
16	W10	4	12	400	19	0	2
17	W10	4	20	200	23	10	4
18	W10	4	30	300	15	3	8

Table 5
Orthogonal experimental combination for move modle 2

No.	A	B	C	D	E	F	H	I
19	W40	1	12	200	15	10	1	0.5
20	W40	1	20	300	19	3	2	1
21	W40	1	30	400	23	0	3	2
22	W40	2	12	200	19	3	3	2
23	W40	2	20	300	23	0	1	0.5
24	W40	2	30	400	15	10	2	1
25	W40	4	12	300	15	0	2	2
26	W40	4	20	400	19	10	3	0.5
27	W40	4	30	200	23	3	1	1
28	W10	1	12	400	23	3	2	0.5
29	W10	1	20	200	15	0	3	1
30	W10	1	30	300	19	10	1	2
31	W10	2	12	300	23	10	3	1
32	W10	2	20	400	15	3	1	2
33	W10	2	30	200	19	0	2	0.5
34	W10	4	12	400	19	0	1	1
35	W10	4	20	200	23	10	2	2
36	W10	4	30	300	15	3	3	0.5

3 Results And Discussions

The abrasive layer of DWS directly affects the quality and efficiency of the slicing process [22]. The abrasive layer of ESDDWS is formed by the repeated superposition of deposition points. The number of deposition points per unit length can characterize the uniformity of abrasive layer distribution of wire saw. We obtained the surface morphology of the saw wire through the optical microscope INSIZE ISM-PM200 (as shown in Fig. 4). According to the calculation formula of the radius of the electric spark discharge channel [19], the diameter of the discharge channel is about 200 μm. Therefore, we assume that the range of a deposition point is the area covered by the circle, in which the diameter is 200 μm. The number of deposition points within the length of the wire saw of 100mm is counted. The results as shown in Table 6 (see Count 1).

On the other hand, the cutting action of DWS is mainly achieved by the exposed diamond abrasives. Therefore, the number of protrusion abrasives grains in the deposition layer is an important factor in evaluating the quality of DWS [23]. The number of protrusion abrasives grains in the deposition layer is counted to evaluate the depositional quality. We use the scanning electron microscope (SEM) COXEM EM-30 Plus to obtain the micro-morphology of the ESDDWS. The micro-morphology of ESDDWS can be divided into four cases (as shown in Fig. 5). (a) The deposition contains only metal materials but no diamond abrasives. (b) The deposition contains diamond abrasives but in small quantities. (c) The deposition contains diamond abrasives with a moderate number of abrasives. (d)The deposition is thicker, and the abrasive particles are heavily accumulated. Due to the abrasive severe accumulated, it is difficult to count the abrasive particles. And it is not good for slicing all the same. In this case, the number of protrusion abrasive grains is counted as 0. The results as shown in Table 6 (see Count 2).

In order to comprehensively consider these two performance indicators, our analysis adopts the comprehensive scoring method. In order to simplify the calculation, we reduce the results of count 1 by 0.02 times as the equivalent score (ES). The scoring table and the extremum difference analysis are carried out (as shown in Tables 6 to 9).

Table 6
Scoring table for move model 1

No.	1	2	3	4	5	6	7	8	9
Count 1	106	288	187	258	212	118	142	172	209
ES	2.12	5.76	3.74	5.16	4.24	2.36	2.84	3.44	4.18
Count 2	0	2	0	1	1	1	0	1	3
Total score	2.12	7.76	3.74	6.16	5.24	3.36	2.84	4.44	7.18
No.	10	11	12	13	14	15	16	17	18
Count 1	192	132	140	246	183	218	219	260	172
ES	3.84	2.64	2.8	4.92	3.66	4.36	4.38	5.2	3.44
Count 2	9	1	8	0	8	4	2	0	1
Total score	12.84	3.64	10.8	4.92	11.66	8.36	6.38	5.2	4.44

Table 7
Extremum difference analysis for move model 1

No.	A	B	C	D	E	F	G
K1	42.84	40.9	35.26	32.66	28.06	30.84	43.38
K2	68.24	39.7	37.94	36	43.9	50.04	40.36
K3		30.48	37.88	42.42	39.12	30.2	27.34
k1	4.76	6.82	5.88	5.44	4.68	5.14	7.23
k2	7.58	6.62	6.32	6.00	7.32	8.34	6.73
k3		5.08	6.31	7.07	6.52	5.03	4.56
R	2.82	1.74	0.45	1.63	2.64	3.31	2.67

According to the extremum difference analysis, in motion mode 1, the sequence of influence of manufacturing parameters is F > A > G > E > B > D > C. And the best combination of process parameters is A2B1C2D3E2F2G1.

Table 8
Scoring table for move model 2

No.	19	20	21	22	23	24	25	26	27
Count 1	162	356	305	333	237	190	272	248	252
ES	3.24	7.12	6.1	6.66	4.74	3.8	5.44	4.96	5.04
Count 2	2	2	1	4	5	1	3	5	5
Total score	5.24	9.12	7.1	10.66	9.74	4.8	8.44	9.96	10.04
No.	28	29	30	31	32	33	34	35	36
Count 1	311	236	175	292	218	195	236	261	318
ES	6.22	4.72	3.5	5.84	4.36	3.9	4.72	5.22	6.36
Count 2	3	3	6	2	7	1	1	7	0
Total score	9.22	7.72	9.5	7.84	11.36	4.9	5.72	12.22	6.36

Table 9
Extremum difference analysis for move model 2

	A	B	C	D	E	F	H	I
K1	75.1	47.9	47.12	50.78	43.92	49.56	51.6	45.42
K2	74.84	49.3	60.12	51	49.86	56.76	48.7	45.24
K3		52.74	42.7	48.16	56.16	43.62	49.64	59.28
k1	8.34	7.98	7.85	8.46	7.32	8.26	8.60	7.57
k2	8.32	8.22	10.02	8.50	8.31	9.46	8.12	7.54
k3		8.79	7.12	8.03	9.36	7.27	8.27	9.88
R	0.03	0.81	2.90	0.47	2.04	2.19	0.48	2.34

According to the extremum difference analysis, in motion mode 2, the influence sequence of manufacturing parameters is C > I > F > E > B > H > D > A. And the best combination of process parameters is A1B3C2D2E3F2H1I3.

The verification experiment is carried out by using the obtained parameter combinations. The micro morphology of ESDDWS by SEM for the verification experiment is shown in Fig. 6. In move model 1, the results of the two indicators are 436 and 10, respectively. In move model 2, the results of the two indicators are 409 and 11, respectively. The results of the validation experiment are better than the original experimental results. However, even under the optimal process combination, there are still the following problems: (1) there are still a considerable number of areas without spark discharge. (2) The deposition point left a pit without deposited materials and abrasives. (3) Material accumulation at the deposition point, especially in motion mode 2. These problems need to be further solved.

4 Conclusion

In this paper, the ESD equipment has been designed according to the characteristics of the ESDDWS process. The discharge gap and supply of electrode material can be adjusted dynamically by SCM.

Orthogonal experiments were carried out for the two motion modes. The number of deposition points on the saw wire and protrusion abrasive particles at the deposit points are used as evaluation indexes. The best combination of the manufacturing process of ESDDWS was obtained under different motion modes by extremum difference analysis. In motion mode 1, the best parameter combination is A2B1C2D3E2F2G1, and the sequence of influence of manufacturing parameters is F > A > G > E > B > D > C. In motion mode 2, the optimal experimental parameter is A1B3C2D2E3F2H1I3, and the influence sequence of manufacturing parameters is C > I > F > E > B > H > D > A. The validation experiment has been carried out. In move model 1, the results of the two indicators are 436 and 10, respectively. In move model 2, the results of the two indicators are 409 and 11, respectively. The results of the validation experiment are better than the original experimental results.

Abbreviations

K_{bond}	Abrasive consolidation ratio (K_{bond} = 1)
L_{dis}	The effective length of single pulse deposition is equivalent to the diameter of the discharge channel (mm)
$N_{discharge}$	The number of times of electrode reciprocating continuous discharge ($N_{discharge}$ = 1)
$N_{duration}$	The number of abrasive particles in the molten droplet after the electrode reciprocates for one time
N_{saw}	The number of abrasive grains consolidated on the substrate after reciprocating deposition
N_{single}	Amount of abrasive particles in melting volume of electrode materials for single pulse discharge
$V_{diamond}$	The volume of diamond (m^3)
V_{melt}	The melting volume of electrode material in single pulse discharge (m^3)
w_t	Mass fraction of diamond particles in the electrode
$\rho_{diamond}$	The density of diamond (3510kg/m^3)
ρ_{mix}	Mixing density of molten droplet of electrode material (8808 kg/m^3)
ρ_{saw}	Abrasive density on saw wire surface (piece/mm)

Declarations

Acknowledgment

This work is financially supported by the National Natural Science Foundation of China (No.52175418, No.51775317); the Key Research and Development Program of Shandong Province, China (No.2019JZZY020209)

Ethical approval

Not applicable

Consent to participate

Not applicable

Consent to publish

The authors declare that this work has not been submitted elsewhere for publication, in whole or in part.

Authors contributions

Chengyun Li is the executor of article writing and experiment operation.

Peiqi Ge contributed to the conception of the work.

Wenbo Bi contributed to the experiment preparation.

Qihao Wang contributed to the equipment design.

Funding

This work is financially supported by the National Natural Science Foundation of China (No.52175418, No.51775317); the Key Research and Development Program of Shandong Province, China (No.2019JZZY020209)

Competing interests

We declare that we have no financial and personal relationships with other people or organizations that can inappropriately influence our work. We have no competing financial interests.

Code availability

Not applicable.

Data availability

The data and materials supporting the results of this article are included within the article.

References

1. Yadlapalli RT, Kotapati A, Kandipati R, Balusu SR, Koritala CS (2021) Advancements in energy efficient GaN power devices and power modules for electric vehicle applications: a review. Int J Energ Res 45(9):12638–12664
2. Wellmann PJ (2017) Power Electronic Semiconductor Materials for Automotive and Energy Saving Applications - SiC, GaN, Ga2O3, and Diamond. Z Anorg Allg Chem 643(21):1312–1322
3. Wang P, Ge P, Bi W, Liu T, Gao Y (2018) Stress analysis in scratching of anisotropic single-crystal silicon carbide. Int J Mech Sci 141:1–8
4. Wang P, Ge P, Gao Y, Bi W (2017) Prediction of sawing force for single-crystal silicon carbide with fixed abrasive diamond wire saw. Mat Sci Semicon Proc. 63, 25-32
5. Kao I, Chung C (2021) Wafer Manufacturing: Shaping of Single Crystal Silicon Wafers. Wiley, First edition. Hoboken, NJ

6. Tsai P, Chou Y, Yang S, Chen Y, Wu C (2013) A Comparison of Wafers Sawn by Resin Bonded and Electroplated Diamond Wire - From Wafer to Cell. IEEE Photovoltaic Specialists Conference. 523-525
7. Furutani K, Murase Y (2008) Fabrication of wire saw with patterned hard bumps by electrical discharge machining with powder suspended in working oil. Manufacturing Systems and Technologies for the New Frontier., pp 361–364
8. Furutani K, Sato H, Suzuki M (2009) Influence of electrical conditions on performance of electrical discharge machining with powder suspended in working oil for titanium carbide deposition process. Int J Adv Manuf Tech 40(11–12):1093–1101
9. Furutani K, Suzuki K (2009) A desktop saw wire coating machine by using electrical discharge machining. IEEE International Conference on Control and Automation ICCA. Christchurch, New Zealand.2165-2170
10. Furutani K, Kanai M, Mieda Y, Suzuki M (2010) Proposal of abrasive layer fabrication on thin wire by electric discharge machining. Int J Automation Technol 4(4):394–398
11. Furutani K, Suzuki K (2015) Experimental investigations of deposition conditions for saw wire fabrication by electrical discharge machining. Int J Adv Manuf Tech 76(9–12):1643–1651
12. Belik VD, Litvin RV, Kovalchenko MS, Rogozinskaya AA (2007) Effect of pulse duration and size of interelectrode interval on electrospark spraying. II. Effect of pulse duration and size of interelectrode interval on composition and mechanical properties of coatings. Powder Metall Met Ceram 46(1–2):95–99
13. Kuptsov KA, Sheveyko AN, Zamulaeva EI, Sidorenko DA, Shtansky DV (2019) Two-layer nanocomposite WC/a-C coatings produced by a combination of pulsed arc evaporation and electro-spark deposition in vacuum. Mater Design 167:107645
14. Frangini S, Masci A (2010) A study on the effect of a dynamic contact force control for improving electrospark coating properties. Surf Coat Tech 204(16–17):2613–2623
15. Wang X, Wang Z, Lin T, He P (2017) Mass transfer trends of A1CoCrFeNi high-entropy alloy coatings on TC11 substrate via electrospark - computer numerical control deposition. J Mater Process Tech 241:93–102
16. Wang X, Wang Z, Lin T, He P (2016) The high-energy micro-arc spark–computer numerical control deposition of planar NURBS curve coatings. Int J Adv Manuf Tech 87(9–12):3325–3335
17. Wang X, Wang Z, He P, Lin T, Shi Y (2015) Microstructure and wear properties of CuNiSiTiZr high-entropy alloy coatings on TC11 titanium alloy produced by electrospark — computer numerical control deposition process. Surf Coat Technol 283:156–161
18. Wang Q, Bi W, Ge P (2018) Developing equipment for electro-depositing diamond wire saw. Diamond Abrasives Eng 38:61–65
19. Li C, Ge P, Bi W (2021) Thermal simulation of the single discharge for electro-spark deposition diamond wire saw. Int J Adv Manuf Tech 114(11–12):3597–3604
20. Li C, Ge P, Bi W (2021) Thermal simulation of the continuous pulse discharge for electro-spark deposition diamond wire saw. Int J Adv Manuf Tech.

21. Mohri N, Saito N, Tsunekawa Y, Kinoshita N (1993) Metal Surface Modification by Electrical Discharge Machining with Composite Electrode. CIRP Annals - Manuf Techno 42(1):219–222
22. Zhao Y, Bi W, Ge P (2021) An on-line inspection method for abrasive distribution uniformity of electroplated diamond wire saw. J Manuf Process 71:290–297
23. Zheng J, Xie Q, Ge P, Meng J, Bi W (2021) Study on the abrasive retention capacity on the surface of electroplated diamond wire saw. Int J Adv Manuf Tech 116(1–2):747–758

Figures

Figure 1

ESDDWS equipment: **a** 3D model; **b** Partial section view

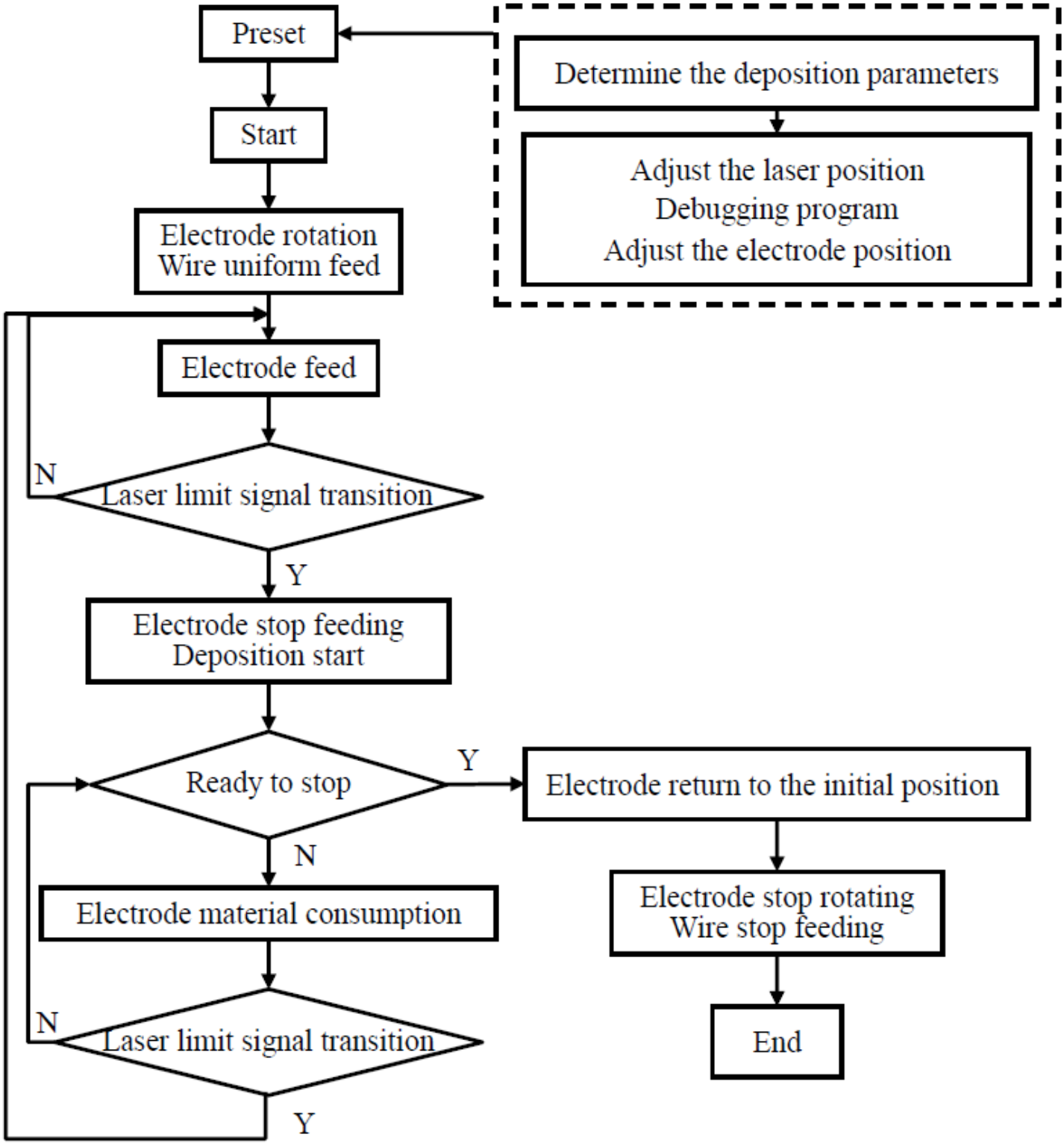

Figure 2

The motion control flow chart of deposition process for move model 1

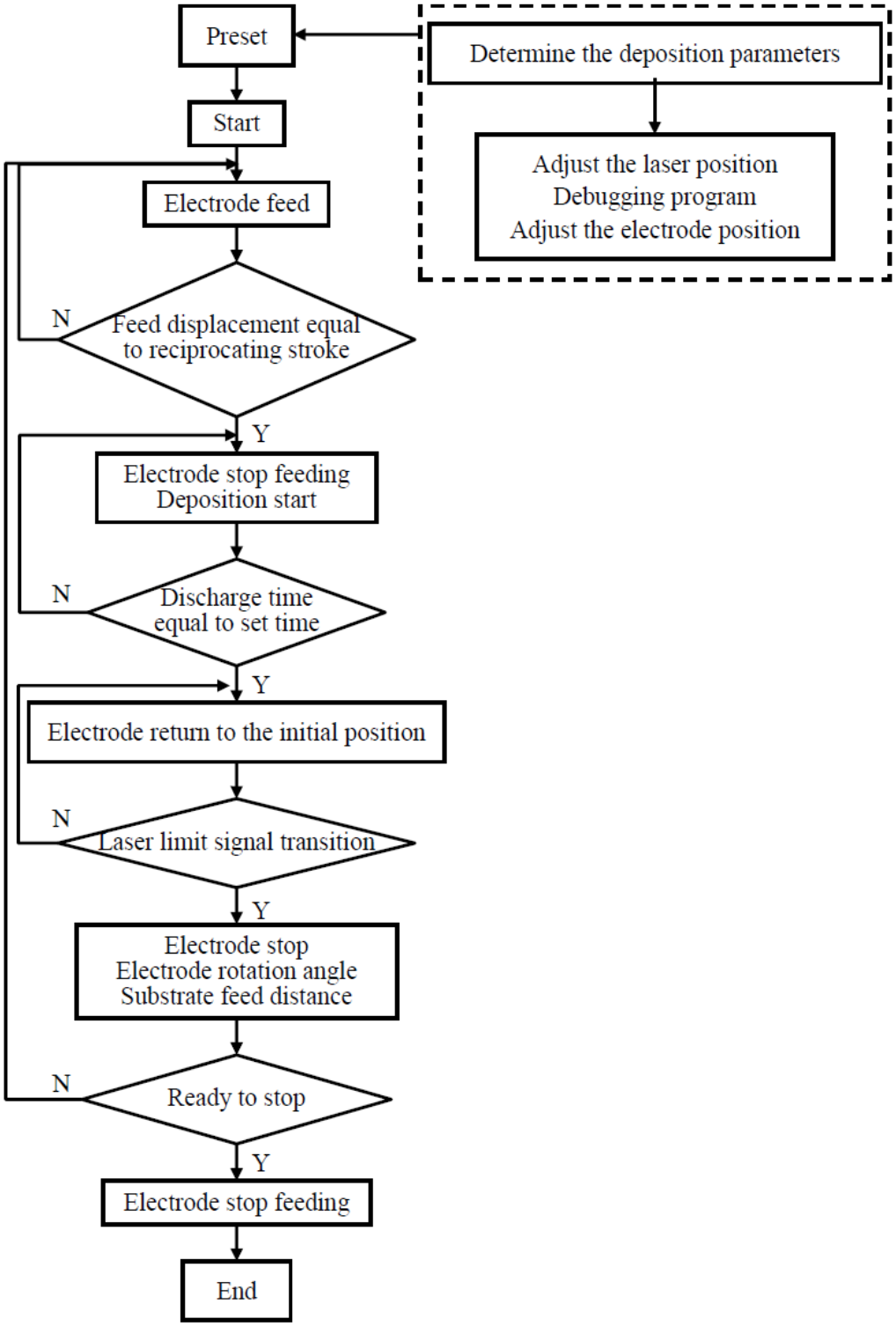

Figure 3

The motion control flow chart of deposition process for move model 2

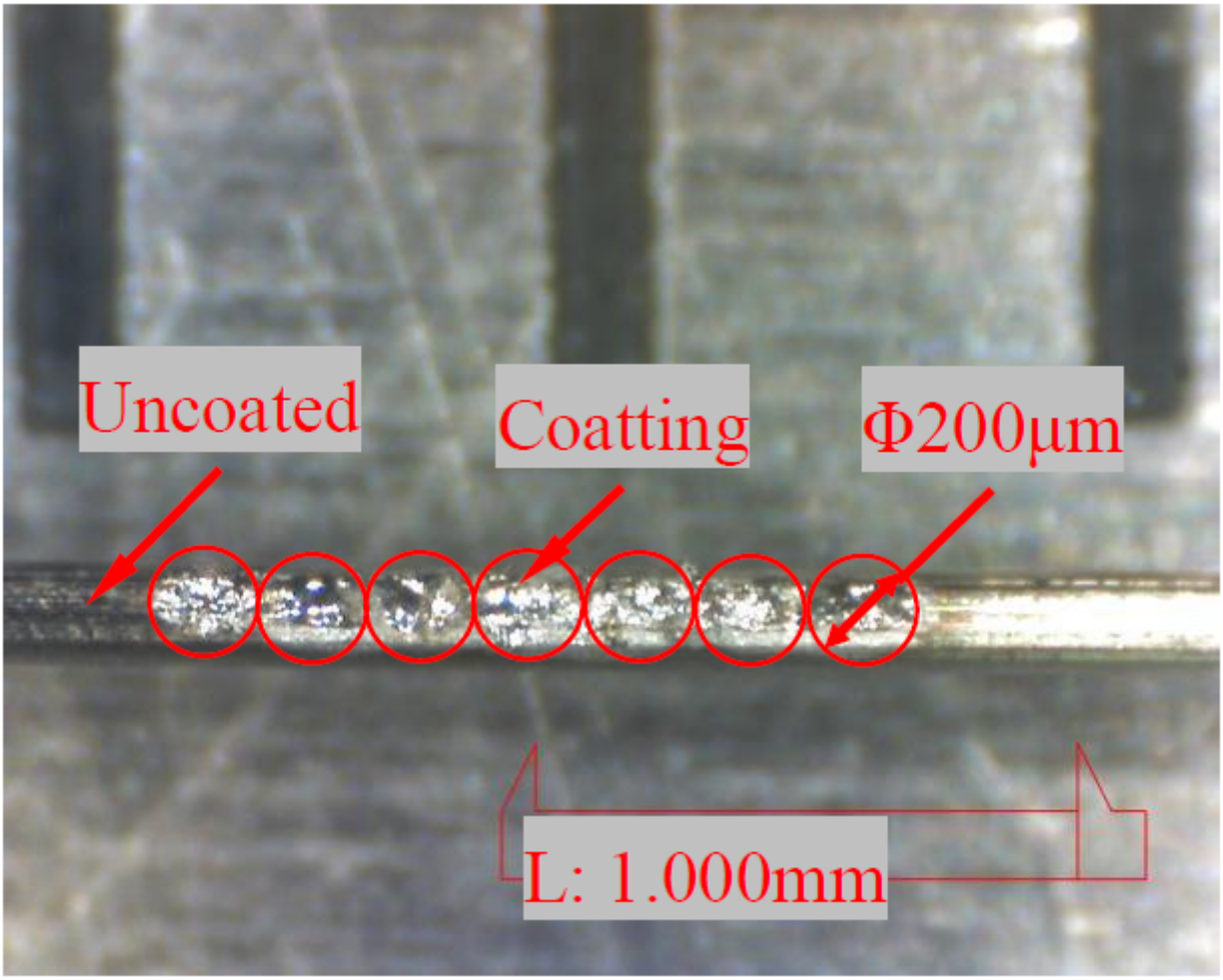

Figure 4

Micro morphology of ESDDWS by INSIZE ISM-PM200

Figure 5

Micro morphology of ESDDWS by SEM

Figure 6

Micro morphology of ESDDWS by SEM for verification experiment: **a** Move model 1; **b** Move model 2